Waste and Biomass Valorization (2022) 13:3767–3786
https://doi.org/10.1007/s12649-022-01797-8

ORIGINAL PAPER

Study of the Crystallisation Reaction Behaviour to Obtain Struvite

Francisco Corona[1,2] · Dolores Hidalgo[1,2] · Jesús María Martín-Marroquín[1,2] · Juan Castro[1] · Sergio Sanz-Bedate[1] · Gregorio Antolín[1,2]

Received: 22 December 2021 / Accepted: 13 April 2022 / Published online: 15 May 2022

Abstract

The potential of N and P recovering from digestate by means of its precipitation in the form of struvite is evident. However, it is necessary to optimise the process at a larger scale, to achieve results that can be extrapolated to evaluate the technical and economic feasibility of the process at an industrial scale. In this work, batch and pilot plant tests were carried out in order to consolidate, at a sufficiently relevant scale, the results obtained at lab scale. For this purpose, the parameters that have the greatest effect on the reaction yield in a fludised bed reactor were selected (Mg and P concentration, flow rate of the fluidising agent (air) and reaction time). Digestate produced in anaerobic digestion plant from pig manure was used as raw material. According to the results obtained, for the struvite crystallisation reaction, the great operational levels for the Mg/P, N/P, air flow rate and reaction time are 1.5, 4.0, 6.0 NL·min^{-1} and 0.5 h, respectively. Finally, a study was carried out to establish the agronomic potential of the salt (struvite) as a biofertiliser in the turf crop, obtaining a similar behaviour of the struvite used in this work to that of commercial struvite.

Graphical Abstract

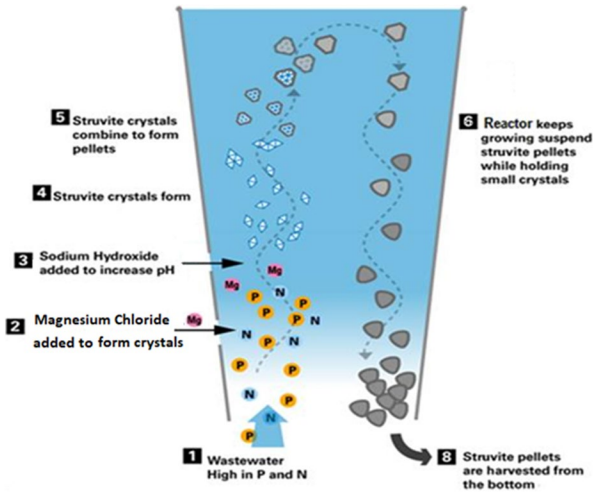

Keywords Crystallisation · Phosphorus · Digestate valorisation · Slow-release fertiliser · Struvite

Statement of Novelty

This article reports on the influence of the main operating parameters on the struvite crystallisation reaction from digestate obtained by anaerobic digestion of pig manure. This is significant because it is one of the most promising

✉ Francisco Corona
fraenc@cartif.es

[1] CARTIF Centro Tecnológico, Boecillo, 47151 Valladolid, Spain

[2] ITAP Institute, University of Valladolid, 47010 Valladolid, Spain

techniques for the nutrient recovery (N and P) from agricultural and livestock wastes. We believe that this manuscript is novel because there is not much work on obtaining struvite from agricultural or livestock waste on a pilot scale. The results obtained can be used for reliable industrial scale-up and integration into currently developed nutrient recovery technologies.

Introduction

Currently, one of the most promising alternatives for phosphorus (P) recovery from wastewater or agro/feedstock waste is the precipitation of Nitrogen N and P in the form of struvite [1–5]. Precipitation of struvite takes place through a crystallisation reaction in which the N and P present in the effluent as NH_4^+ and PO_4^{3-} react with an external source of magnesium (Mg) to produce a salt of magnesium ammonium phosphate (MAP):

$$Mg^{2+} + NH_4^+ + PO_4^{3-} + 6H_2O \rightarrow MgNH_4PO_4 \cdot 6H_2O$$

The effectiveness of struvite precipitation as a nutrient recovery technology is largely affected by the kind of crystalliser, as well as its operating regime, for which two main aspects are considered: P removal performance and product composition. So far, research to recover P from waste effluents by struvite precipitation has focused on using stirred reactors (SR) [6, 7] and, to a lesser extent, in fluidised bed reactors (FBR) [8, 9], either air or liquid fluidising. An SR is simple to operate and often achieves high P removal yields, but has the disadvantage of producing fines during the crystallisation reaction mainly due to the high level of mixing at which it is usually operated, resulting in contamination of the crystal by the inclusion of these fines [10]. On the other hand, when an FBR is used, there is the advantage that the struvite crystals produced will possess optimal properties for use as biofertilisers with desirable qualities [11] (struvite crystals should be of the required size to be dosed by agricultural machinery, as well as the required purity and nutrient composition to be able to substitute mineral fertilisers.). Cylindrical FBRs can now be found whereby P and N can be recovered, yielding high purity struvite pellets up to several millimetres in size [11, 12], as the size of the crystal will be influenced by fluid dynamics. This technology prevents the spontaneous precipitation of salt in wastewater treatment plants, which can lead to clogged pipes, and produces a biofertiliser with a particle size suitable for use, which is both environmentally and economically beneficial [13]. However, although FBRs have the benefit of obtaining struvite crystals of a larger size, the P removal performance is sometimes lower than that obtained by SRs. This is because to produce a correct mixing of the raw material, a high speed of the fluidising agent is necessary, which can lead to the dragging of fines from the struvite crystals (fines) [11, 14]. Currently the most interesting alternatives to control the appearance of fines are to include a filtration, clarification [15, 16] or agglomeration using coagulants.

Taking into account the fundamentals of crystallisation reactions, the factors that most influence the growth of crystalline nuclei are hydrodynamic and thermodynamic [17, 18]. Thus, a nuclei can grow to form a larger crystal or it can be formed by the union of several nuclei (aggregate) [19]. Thus, it is possible to control crystal growth and aggregate formation, by optimising the hydrodynamic and thermodynamic parameters, avoiding the formation of fines.

Many works demonstrate that, in addition to the kind of reactor used, there are several factors that greatly influence crystal formation [20]. Among the factors, the saturation index is the most important, is strongly influenced by the presence of the species that will participate in the reaction (Mg, P and N concentration) and the pH level of the corresponding solution [21, 22]. In addition, other variables, i.e. temperature, foreign substances or the intensity of mixing (for SR reactors) have also been shown to be influenced to a lesser extent [23–25]. Thus, pH and temperature are parameters that influence the induction time of the crystallisation reaction, as well as the solubility of the medium and thus the precipitation of crystals. According to Mehta & Batstone [17], an increase in pH and temperature represents a reduction in induction time, as well as an increase in solubility in the case of temperature and a decrease in the case of pH (although the latter depends on the working pH levels). The presence of foreign ions can interfere with the crystallisation mechanism, as well as decrease the reaction yield by competitive reactions in the medium. The intensity of mixing directly influences the rate of crystal growth. However, recent studies recognise that struvite precipitation yield and particle size, for FBR reactors are largely related to the rate or flow rate of the fluidising agent and the retention time of the crystals [11, 26, 27].

Thus, the objective of this study is to assess the influence of the key parameters of the struvite crystallisation reaction process (Mg and P concentrations, fluidising agent flow rate and retention time) from anaerobic digestion (AD) digestate using a pilot-scale FBR.

Materials and Methods

Crystallisation Experiments

Experiments for the study of struvite crystallisation at pilot scale were carried out in batch mode in a 50 L volume FBR. All reactions were carried out at pH 9.0 and 25 °C temperature. These values were selected, taking into account the

results obtained at laboratory level [28] as the most optimal under economical and technical perspective, since, at higher values of temperature and pH, better results are obtained, but most of the N contained in the digestate is lost in the form of gaseous ammonia, which prevents its recovery in the form of struvite. Moreover, different residence times (0.5, 1.0 and 2.0 h) and fluidising agent flow rates (2.0, 6.0 and 12.0 $NL{\cdot}min^{-1}$) were studied. Digestate obtained from a pig slurry AD plant in Almazán (Spain) was used in all experiments. The content of the different nutrients in the digestate is shown in Table 1.

Before crystallisation, the samples were subjected to a solid–liquid separation step by centrifugation, in order to eliminate the solids that the digestate might contain, and thus favor the mixing of the reagents to produce the struvite crystallisation and avoid fouling and blockages in the reactor. The centrifugation of the samples was carried out with a GEA Westfalia OTC 3-03-107 centrifuge.

A FBR of own design (Fig. 1) was used for the pilot scale tests of the study carried out in this chapter. It is a 50 L working volume reactor made of borosilicate glass with a cylindrical shape. The reactor has an internal diameter of 20 cm and a total height of 2 m, so that the L/D ratio = 10 recommended for FBRs is achieved. Inside the reactor is a methacrylate cylinder with a diameter of 10 cm and a height like the outer cylinder. The reactor has four peristaltic pumps for dosing the raw material (digestate) and the required reagents (Mg salt, P salt and NaOH). In the lower part of the reactor there is a diffuser for the introduction of air, which acts as a fluidising agent for the medium and for its homogeneous dispersion.

Once the sample was centrifuged, the digestate and the necessary amount of Mg salt and P salt (depending on the experiment) were added to the reactor, so that each sample had its corresponding N/P and Mg/P molar relationship (Table 2). The Mg salt used was $MgCl_2{\cdot}6H_2O$, while the P salt was $Na_2HPO_4{\cdot}12H_2O$, both of technical grade. The

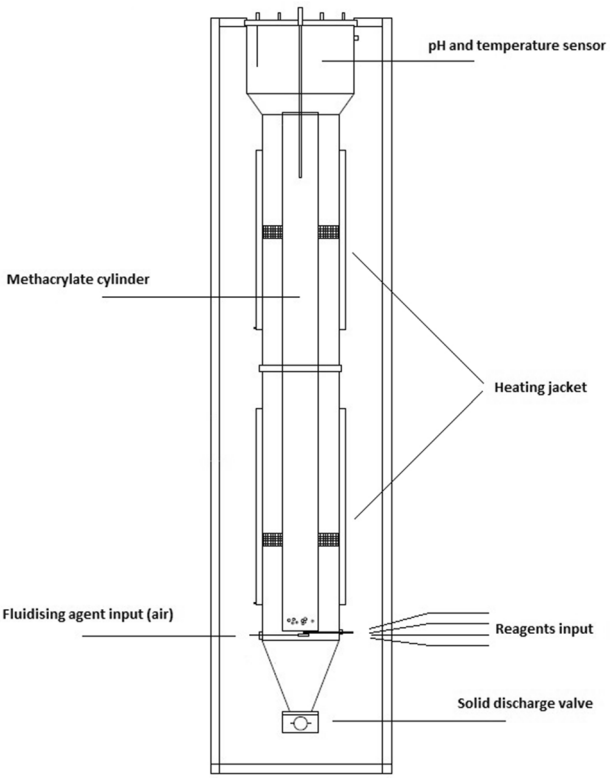

Fig. 1 Schematic of the fluidised-bed crystallisation reactor

amounts of Mg and P salt added have been calculated taking into account the initial concentration of these elements in the initial digestate sample. The amount of N, Mg and P in the digestate is known, the amount of N is fixed (as it will not be added from an external source), so taking into account the number of N and the N/P ratio, the amount of total P required was calculated. Therefore the amount of P salt added resulted from the difference between the amount of total P required and the amount of initial P present in the digestate. Subsequently, an analogous process was carried

Table 1 Nutrient content the digestate

Test #	NH_4^+-N ($mg{\cdot}L^{-1}$)	P_T-P ($mg{\cdot}L^{-1}$)	Mg^{2+} ($mg{\cdot}L^{-1}$)	Ca^{2+} ($mg{\cdot}L^{-1}$)
1	3383.28	239.69	–	5.80
2	3328.01	211.85	–	7.95
3	3368.12	182.64	–	–
4	3508.66	270.46	–	24.98
5	3708.57	228.76	–	9.58
6	3926.87	182.21	–	16.91
7	3693.47	198.02	–	11.32
8	3602.18	206.86	–	–
9	3854.84	210.81	–	–

–: not detected

Table 2 $MgCl_2{\cdot}6H_2O$ and $NaH_2PO_4{\cdot}12H_2O$ amounts for each test

Test #	Mg/P molar ratio	N/P molar ratio	$MgCl_2{\cdot}6H_2O$ amount (g)	$NaH_2PO_4{\cdot}12H_2O$ amount (g)
1	1.0	4.0	613.22	943.41
2	1.0	8.0	301.60	409.72
3	1.0	12.0	203.49	253.51
4	1.5	4.0	953.92	965.73
5	1.5	8.0	504.13	460.80
6	1.5	12.0	355.87	313.31
7	2.0	4.0	1338.88	1066.67
8	2.0	8.0	652.90	456.44
9	2.0	12.0	465.79	289.11

out with the Mg salt. Finally, the pH of the samples was around 8.5, so the addition of a concentrated alkali (50% w/w NaOH solution) was necessary to raise the pH value to 9.0.

After the reaction time had elapsed, the crystal harvest was collected by means of the solids discharge valve and the sample was concentrated by centrifugation to obtain the struvite crystals formed. A centrifuge model Jouan model B4i was used in the operation. The sedimented phase (crystals) was subjected to a drying process in an oven at 40 °C for 48 h, to remove moisture. Higher temperatures were not used since the crystalline structure of struvite can be altered for temperatures above 50 °C [29]. Moreover, the supernatant obtained from centrifugation (crystallisation mother liquor) was removed for subsequent analysis of N, P and Mg concentration.

Once these experiments were completed, they were repeated maintaining the same levels and factors, but increasing the pH and the reaction temperature to 10.5 and 35 °C. The purpose of these experiments was to know the influence of temperature and pH parameters on the NH_3/NH_4^+ equilibrium at pilot scale.

All experiments were carried out in duplicate, eliminating outliers.

Agronomic Tests

Once the struvite crystallisation tests were completed, a field trial was carried out to determine its agronomic power. For this purpose, a circular plot of 3 m^2 was selected and divided into three sectors of 1 m^2. In all the sectors, conventional turf was planted and in one of them a traditional fertiliser (TF) was added, in another one commercial struvite (CS) and in the last one, the experimental struvite obtained in this work (ES). The TF used is a N-P-K (22-5-10) slow-release fertiliser especially indicated for turf, while the commercial struvite is the Crystal Green® product. As a reference in the dosage in the three cases, 18 g N m^{-2} soil was taken. Fertiliser dosing was carried out in a single step. Table 3 shows the fertiliser composition and dosage. After 22 weeks, when the turf had grown to a sufficient height, both soil and turf were sampled in each of the sectors for analysis.

Table 3 Composition and dosage of fertilisers

Kind of fertiliser	N content (%w)	P content (%w)	Mg content (%w)	Fertiliser dosage (g m^{-2})
Traditional fertiliser (TF)	22	2	1	81.8
Commercial struvite (CS)	5	10	9	386.3
Experimental struvite (ES)	5	9	8	363.6

Analytical Methodology and Instrumentation Used in Analysis

All the analytical techniques that have been applied in this study to carry out the characterisations of the process streams in each of the experiments and agronomic tests, are been shown by Corona et al. [28].

Fresh digestate samples were obtained from an AD plant in Almazan (Spain). Fresh digestate was stored at 4 °C in a refrigerator until it was used. For the characterisation of the samples, Nitrogen was measured by titrimetric method using a distiller (Selecta, RAT 2), a digester (Selecta) and a digital burette (Bran). Total P was determined by vanadomolybdophosphoric acid spectrophotometry in a Shimadzu UV–VIS spectrophotometer, model UV-1603 and a Selecta digester, model RAT 2. Mg concentration was analysed with an inductively coupled plasma optical emission spectrophotometer (ICPOES) (Shimadzu AA-6800, Japan). The analyses have been carried out following the current standard for water analysis in Spain (AENOR 2002; AENOR 2005; Apha A 2000). pH was determined by a potentiometric method using a Crison pH meter, model pH 25. Reagents used and struvite samples obtained were weighed using a Sartorius model TE 214S analytical balance. The dry solid fraction of the initial digestate was obtained by drying at 105 °C for 48 h using a Selecta Digitronic model stove. Separation of the liquid and solid fractions of the samples used in the experimentation was carried out by centrifugation at 5000 rpm for 10 min using a Jouan model B4i centrifuge. The reagents used in this work have been $MgCl_2{\cdot}6H_2O$ (Scharlau brand, pure grade). The characteristics and morphology of the crystals were obtained by a scanning electron microscope (SEM) analysis (FEI QUANTA 200). By means of X-ray diffraction (XRD), the qualitative identification of the mineralogical composition of the crystalline sample was carried out. A Bruker diffractometer model D8-Advance with Göebel mirror was used to carry out the analyses. Angle 2θ (diffraction angle) scans were collected from 5° to 75°, with a of 2θ stepwidth of 0.05 and a sampling time of 3 s per step. The qualitative identification of the sample was done with the ICDD (International Center for Diffraction Data) database, being 01-071-2089, for the struvite. Crystal particle size determination was carried out using a Beckman Coulter model LS200 laser diffraction particle size distribution equipment. The reference followed in this case was the methodology developed by the provider itself. The methodology follows the MIE theory or Fraunhofer theory, according to which the data of the light scattered by a set of particles is transformed into a size distribution by using an algorithm that uses known diffraction patterns for particles in the range that is measured.

Theory and Calculation

Taguchi Methodology for Design of Experiments

Once the process under study was established, the operating parameters (factors) that were most important to the development of the process were defined and the work levels for each of the parameters were specified.

Given the large number of parameters involved in the process, as well as their interrelationship, a design of experiments (DOE) was carried out, in order to allow the number of experiments to be reduced to a minimum without losing relevant information. The choice was made to carry out the DOE following the Taguchi methodology.

In order to apply the Taguchi methodology, the P removal from the reaction and the particle size were identified as output variables. For both variables, the type of optimisation sought was larger-better, i.e., the P removal yield and crystal size were sought to be as large as possible.

The control factors selected were Mg influence (Mg/P relationship), P influence (N/P relationship), fluidising agent flow and reaction time. This selection is mainly since these are the parameters that mainly affects the struvite saturation index (concentration of species in the reaction medium) and on the other hand these are the factors that most affect the fluidised bed reaction (reaction time and flow rate of the fluidising air). All factors were tested at three levels. Table 4 shows a summary of the DOE proposed for the study in this work.

Full factorial design was reduced to L_9 orthogonal array by Taguchi methodology. By this reduced design, four parameters at three levels have been researched, implementing nine experiments (Table 5).

Minitab 17 has been the software used to the definition of the DOE and the statistical analyses of the results.

P removal yield

The P removal yield shall be calculated as given by Eq. (1).

$$P\ removal\ yield(\%) = \frac{\left[(solid\ crystal\ mass)\cdot\left(\%\frac{w}{w}\Big/100\right)_P\Big/M_P\right]}{(initial\ moles)_P}\cdot 100 \quad (1)$$

Table 4 DOE for struvite crystallisation at pilot level

Parameters	Levels		
Mg/P molar ratio	1.0	1.5	2.0
N/P molar ratio	4.0	8.0	12.0
Air flow (NL·min^{-1})	2.0	6.0	12.0
Reaction time (h)	0.5	1.0	2.0

Table 5 L_9 orthogonal DOE for pilot plant study

Test #	Mg/P molar ratio	N/P molar ratio	Air flow (NL·min^{-1})	Reaction time (h)
1	1.0	4.0	2.0	0.5
2	1.0	8.0	6.0	1.0
3	1.0	12.0	12.0	2.0
4	1.5	4.0	6.0	2.0
5	1.5	8.0	12.0	0.5
6	1.5	12.0	2.0	1.0
7	2.0	4.0	12.0	1.0
8	2.0	8.0	2.0	2.0
9	2.0	12.0	6.0	0.5

where M_P is the atomic mass of P (30.97 g mol^{-1}). Solid crystal mass is the mass of solid crystal obtained after the struvite reaction, the centrifugation concentration step and the drying step (final solid product). (%w/w) is the weight fraction of P in the final solid product.

Nitrogen lost as NH_3

As can be seen in Eq. (2), the amount of N lost as gaseous NH_3 has been determined by a balance to that element:

$$\left(\text{moles removed as } NH_3\right)_N = (\text{initial moles})_N - (\text{mother liquor moles})_N - (\text{solid crystal moles})_N \quad (2)$$

Thus, the percentage of N lost as NH_3 will be:

$$N\ lost\ as\ NH_3(\%) = \frac{\left(moles\ removed\ as\ NH_3\right)_N}{(initial\ moles)_N}\cdot 100 \quad (3)$$

Mass Balances of Mg and P

The amount of Mg or P in the crystal can be known directly, as shown in Eq. (4).

$$(\text{mass obtained as solid crystal})_i = (total\ mass\ of\ crystal)\cdot\left(\%\frac{w}{w}\Big/100\right)_i \quad (4)$$

where i is either Mg or P in each case.

Moreover, unlike N, in the case of P and Mg there are no loss of matter in the form of gas. Therefore, by carrying out a balance to Mg or P, the amount of these two elements in the crystal can be determined, since the initial amounts of Mg and P and the remaining amounts of both in the mother liquor after crystallisation are known.

$$(\text{mass obtained as solid crystal})_i = (\text{initial mass in digestate})_i - (\text{mass of mother liquor})_i \quad (5)$$

where i is either Mg or P in each case.

Therefore, the result obtained by Eq. (5) can be used to determine the error in the closure of the balance associated with P:

$$(\text{Error})_P(\%) = \frac{(\text{solid crystal mass according Eq 5})_P - (\text{solid crystal mass according Eq 4})_P}{(\text{solid crystal mass according Eq 5})_P} \cdot 100 \quad (6)$$

Results

Table 6 shows the results obtained (P removal yield and particle size) for each test.

Table 6 Test results

Test #	P removal yield (%)	Particle size (μm)
1	84.62	100.72
2	80.30	102.95
3	77.86	146.25
4	90.03	106.33
5	89.74	118.32
6	86.03	132.33
7	91.29	104.50
8	88.78	104.31
9	88.15	122.42

Crystallisation Study at Pilot Scale

Effect of Mg Concentration

The effect of Mg concentration on P removal yield is shown in Fig. 2 using the Mg/P molar relationship. P removal yield generally increases with the Mg/P ratio rising. However, the reaction yields are very similar when using Mg/P ratios of 1.5 and 2.0. As far as particle size is concerned, no clear trend can be observed, although maximum values are obtained for certain experiments with Mg/P relationships of 1.0 and 1.5.

Influence of P

According to Fig. 3, in general, there is an inverse relationship between the P removal yield and the N/P molar relationship, since, as the value of the N/P molar relationship increases, the P removal yield decreases. However, with regard to particle size, the opposite trend is observed for P removal yield, i.e. in general, the particle size increases as the N/P molar relationship increases.

Influence of Fluidisation Air Flow Rate

With some exception, the P removal yield rises with increasing air flow rate (Fig. 4). The largest particle sizes are found at the lowest values of fluidising agent flow rate (2 and 6 $NL{\cdot}min^{-1}$), with one important exception, the maximum particle size value (146.25 μm) was obtained in an experiment with maximum fluidising agent flow rate (12 $NL{\cdot}min^{-1}$).

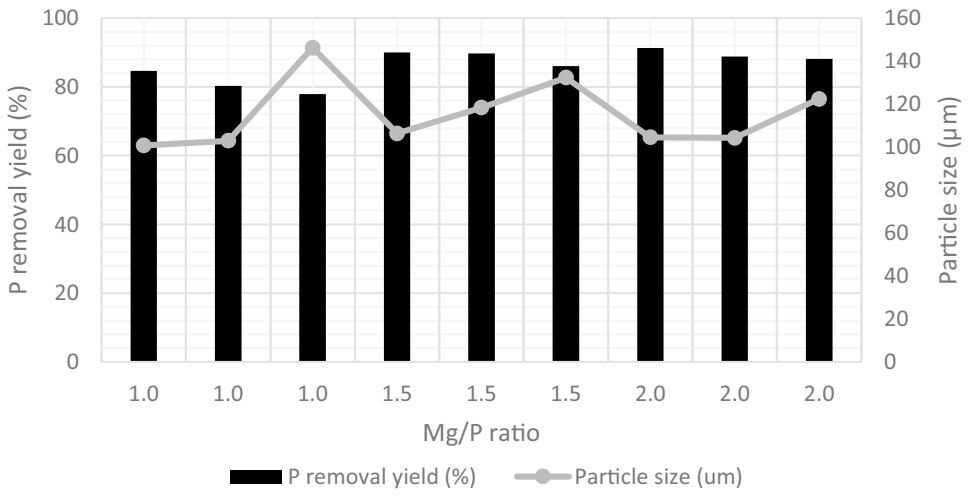

Fig. 2 Effect of Mg/P on P removal and particle size at pilot scale

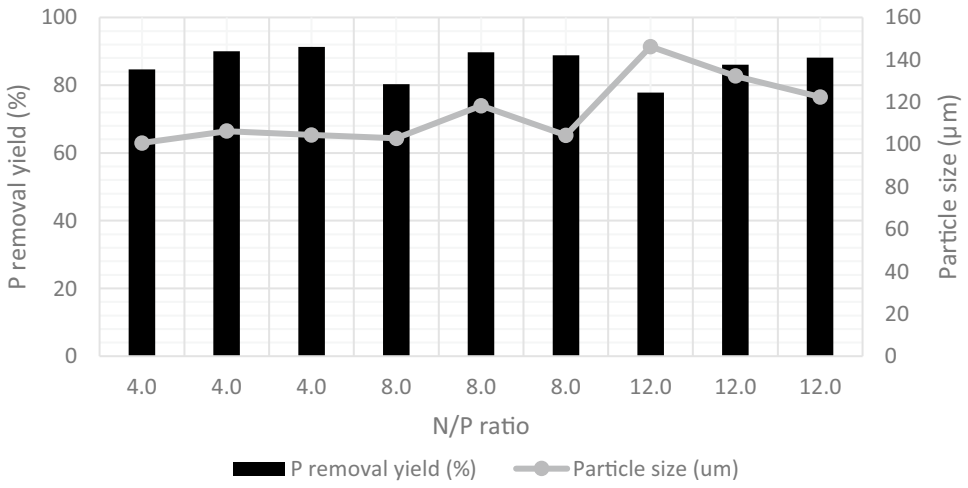

Fig. 3 Effect of N/P on P removal and particle size at pilot scale

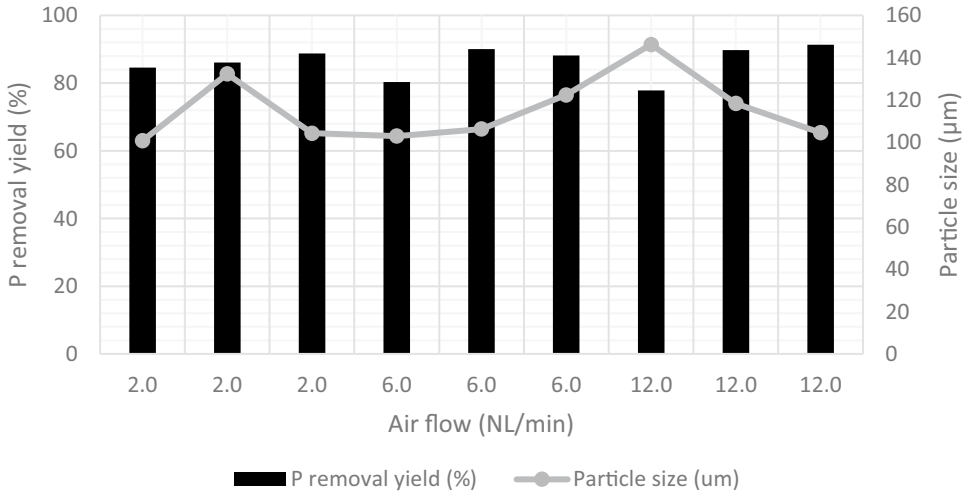

Fig. 4 Effect of air flow rate on P removal and particle size at pilot scale

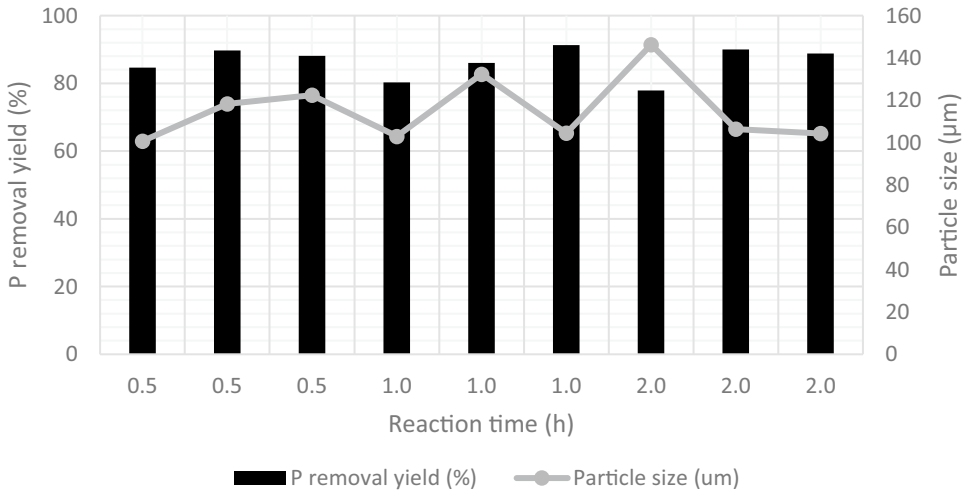

Fig. 5 Effect of reaction time on P removal and particle size at pilot scale

Table 7 Results of experiments at pilot scale

Test #	N lost as NH_3 (%)
1	71.65
2	90.27
3	68.36
4	77.63
5	85.46
6	67.00
7	85.90
8	75.72
9	74.37

Temperature 35 °C and pH 10.5

Influence of Reaction Time

In this case, the P removal yield does not show a uniform evolution (Fig. 5). The maximum yield values are obtained at the 1.0 and 2.0 h reaction time. For these two reaction times the differences in P removal yield are very small. Regarding the particle size, no clear relationship can be appreciated, but the values obtained are similar for the lower reaction times (0.5 and 1.0 h) and slightly higher when the residence time is 2 h.

Effect of Temperature and pH on the Chemical Equilibrium of NH_3/NH_4

To know the influence of pH and temperature on the NH_3/NH_4^+ chemical equilibrium, new test were achieved with identical levels of Mg/P molar relationship, N/P molar relationship, air flow rate and reaction time, but in all cases the pH was increased to 10.5 (instead of 9.0) and the reaction temperature to 35 °C (instead of 25 °C). The results of the percentage of N lost as NH_3 are shown in Table 7.

It is evident that the N loss increased drastically compared to the reactions where lower pH and temperature were used.

Crystal Habit of Struvite

A picture by scanning electron microscope (SEM) of the struvite crystals obtained using the pilot scale FBR is presented in Fig. 6. As can be seen, the habit of the obtained crystals have the characteristic shape of struvite crystals, i.e. needle-shaped crystals.

The diffractogram for struvite has been contrasted with an XRD pattern (01-071-2089), which has been obtained from the equipment software library. As can be seen in Fig. 7, the diffractogram of the struvite obtained in this work presents well defined and clean peaks. On the other hand, in the lower part of Fig. 7, the diffractogram is superimposed with the lines of the struvite standard peaks. Thus, no representative variations in the peaks (both in intensity and position) are observed between the diffractogram of the struvite sample and the standard. The latter implies that the crystals produced by the crystallisation reaction are struvite and that the purity of the struvite is quite high, although some amorphous growth is occasionally found (as can be seen on the right side of Fig. 6), which mainly corresponds to the formation of calcium precipitates (due to the presence of the foreign ion in the reaction sample).

Agronomic Potential of Struvite

Table 8 shows the characterisation of the soils and turf in each of the sectors under study.

In the case of soils, all three have very similar characteristics, both for micronutrients and metals. The major differences shown are: (1) Ca, Na and Zn concentration. These are considerably higher for soil fertilised with CS. (2) Concentration of Si and Ba. These metals have much higher concentration values in soil fertilised with struvite than in soil fertilised with TF. (3) Concentration of Sr. Metal with a notably higher concentration in the TF soil than in the struvite soils. As far as Ca and Na are concerned, the explanation may be that struvites have small amounts of these elements as impurities. This is not the case for Zn, Si, Ba, Sr. The struvites do not contain significant amounts of these metals, therefore, their slightly higher concentration in soils where struvites have been dosed may be due to the intrinsic presence of these substances in the corresponding soil sector.

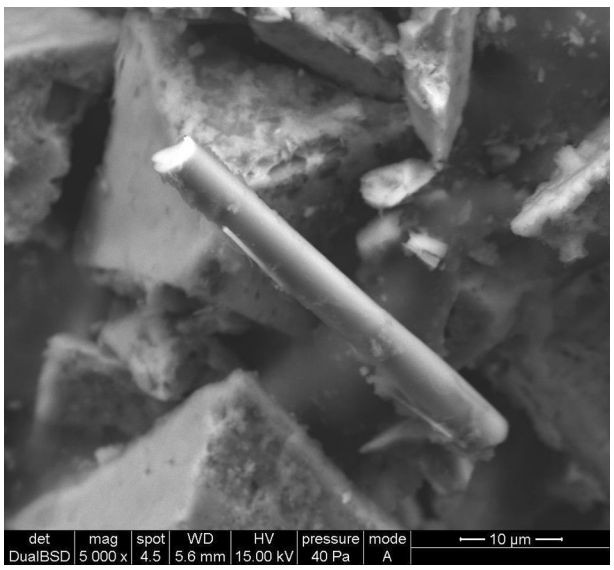

Fig. 6 Picture obtained by SEM image of the crystals

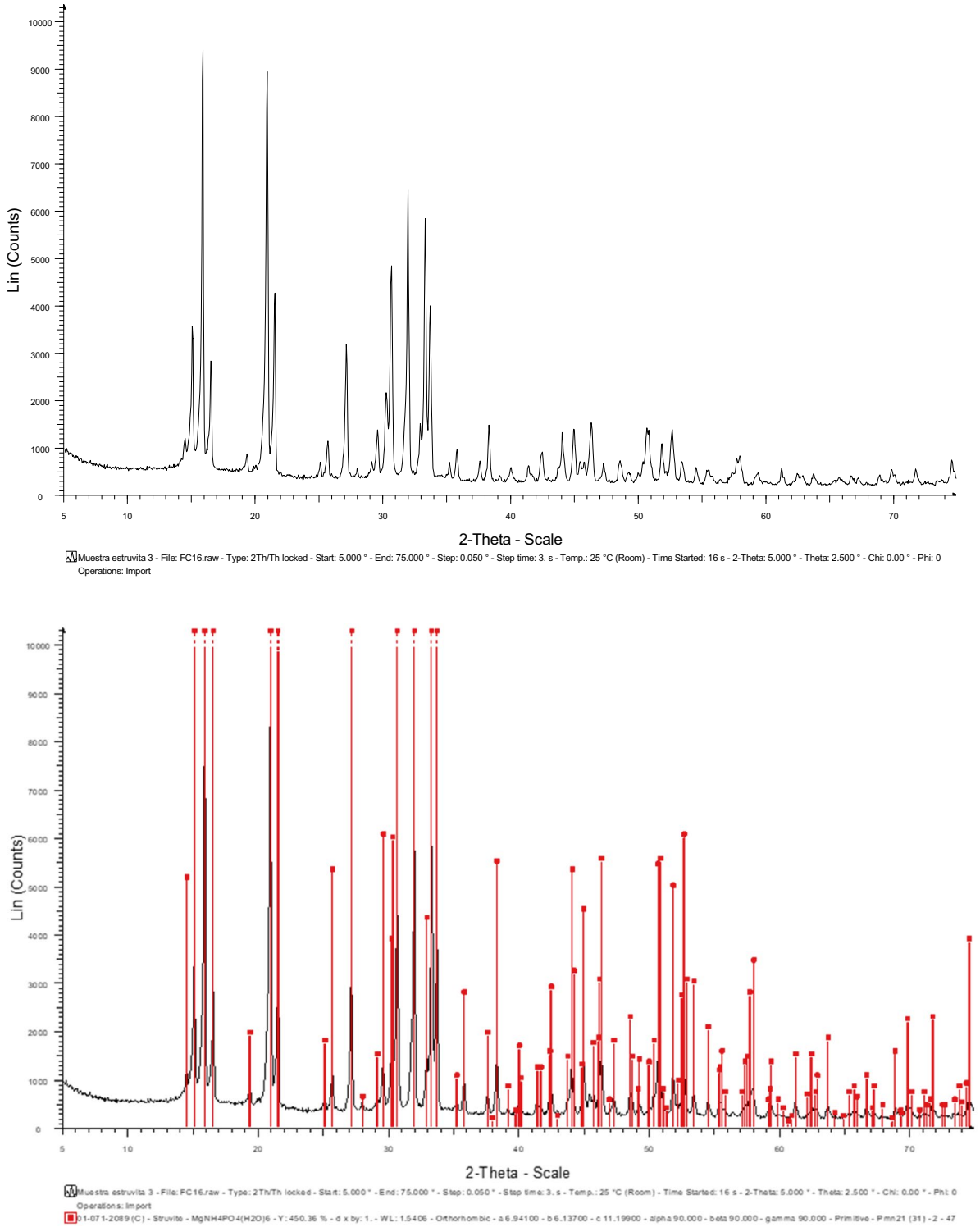

Fig. 7 Diffractogram of the struvite obtained in the pilot scale experiments

Moreover, the concentrations found in the turf that have grown in each of the sectors under study have very similar characteristics. The major differences are found in: (1) Concentrations of Si, Cu and Mn. Metals with higher concentrations in the turf obtained in the sector where the TF was used. (2) Concentration of Sr. This metal has a higher concentration in the turf from the CS sector. (3) Zn concentration. The Zn content is slightly higher in the turf

Table 8 Soil and turf composition for each of the fertilisers (dry basis)

Test #	Soil TF	Soil CS	Soil ES	Turf TF	Turf CS	Turf ES
Carbon (%w)	2.7	2.3	1.1	44.0	45.1	44.8
Hydrogen (%w)	0.8	0.9	0.7	6.7	6.6	6.8
Nitrogen (%w)	0.21	0.42	0.36	4.59	5.36	5.04
Aluminum (%w)	0.013	0.011	0.015	–	–	–
Calcium (%w)	0.563	0.875	0.631	0.247	0.285	0.285
Iron (%w)	0.008	0.007	0.009	–	0.000	–
Magnesium (%w)	0.522	0.566	0.625	0.204	0.333	0.339
Phosphorus (%w)	0.060	0.068	0.065	0.600	1.008	0.972
Potassium (%w)	0.504	0.513	0.514	1.691	1.734	1.651
Silcom (%w)	0.299	0.506	0.513	0.112	0.035	0.093
Sodium (%w)	0.054	0.072	0.043	0.049	0.057	0.059
Titanium (%w)	0.001	–	–	–	–	–
Barium (ppm)	0.053	0.201	0.191	–	0.200	–
Cadmium (ppm)	–	–	–	–	–	–
Cobalt (ppm)	–	–	–	–	–	–
Chrome (ppm)	0.116	0.083	0.089	0.051	–	–
Copper (ppm)	0.016	0.099	–	0.061	0.004	0.011
Manganese (ppm)	1.555	1.365	1.565	0.476	0.280	0.314
Molybdenum (ppm)	–	–	–	–	–	–
Nickel (ppm)	–	–	–	–	–	–
Lead (ppm)	–	–	–	–	–	–
Antimony (ppm)	–	–	–	–	–	–
Strontium (ppm)	0.442	0.399	0.383	0.256	0.338	0.269
Vanadium (ppm)	0.027	–	0.037	–	–	–
Zinc (ppm)	0.314	0.479	0.257	0.491	0.578	0.583

–: not detected

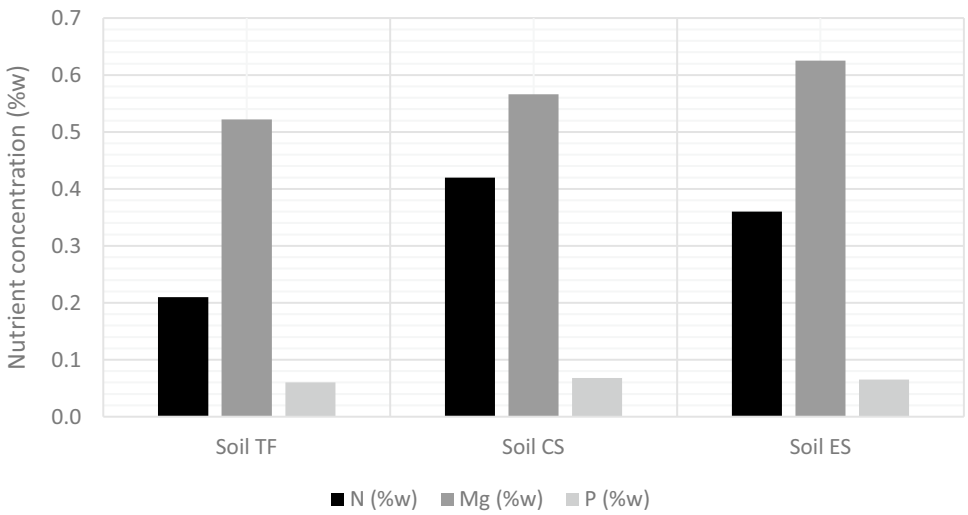

Fig. 8 Nutrient concentration in the different soil fractions (dry basis)

in the CS sector. As mentioned above, no quantities of Si, Cu, Mn, Sr or Zn were detected in any of the three fertilisers used, so that the difference in the absorption of these elements by the grass in each of the sectors is due to the synergic or antagonistic effect of the fertiliser and the absorption of each metal by the plant.

Finally, the differences in the main nutrients supplied (N, P, Mg) are presented in more detail for the three soil and turf fractions. As can be seen in Fig. 8, there are notable differences in the nutrient content in the soils of the three sectors in which the agronomic study was carried out. N is present in a higher proportion in the soil fraction corresponding to

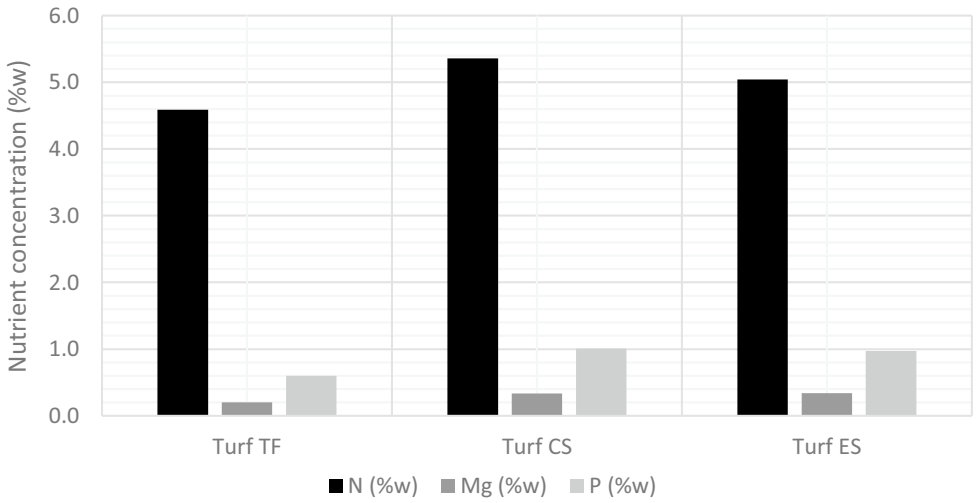

Fig. 9 Nutrient concentration in the different turf fractions (dry basis)

the CS fertilisation zone (0.42% w/w), which is twice the concentration of N in the soil of the TF (0.21% w/w) and much higher than the concentration in the soil of the ES (0.36% w/w). With regard to Mg, the differences are less marked, the concentration of Mg in the soil to which the ES was added being around 0.1% w/w higher (0.63% w/w) than the concentrations for the same metal in the other two soils (0.52 and 0.57% w/w). Finally, the P concentration is again higher in the soil fertilised with CS (0.068% w/w), but with minor differences compared to the other two cases (0.060 and 0.065% w/w). The amount of nutrients available in the sectors where struvites have been dosed is higher. This is explained by the slow-release fertiliser characteristics of struvite. In other words, the fertiliser releases nutrients according to the plant's needs.

As far as turf is concerned, Fig. 9 shows the differences in N, Mg and P concentrations for each of the crops grown in each of the sectors. For N, there are not excessive variations, representing the maximum concentration of this element for the turf obtained from CS (5.36% w/w). The concentration of Mg is very similar in the turf obtained from the two struvites (0.33 and 0.34% w/w) and around 60% higher than the concentration of Mg in the turf obtained from the TF (0.20% w/w). Finally, the trend in P is quite similar to that of Mg, with very similar concentrations in the turf obtained from CS (1.01% w/w) and in the turf obtained from CS (0.97% w/w) and in turn much higher than the concentration of P in the turf from TF (0.60% w/w). As with the soil, turf fertilised with struvite will have a higher nutrient content (N, P, Mg), because, on the one hand, struvite has a higher concentration of P and Mg than TF and, on the other hand, the slow release effect of struvite means that the plants assimilate the nutrients better and in greater quantities.

Discussion

In this paper, the influence of the different factors of the process under study on the struvite P removal yield and the crystal particle size was determined on a pilot scale. The criterion used to quantify the influence has been the signal-to-noise relationship (S/N). Thus, for the DOE implemented in Minitab, the mean of the S/N relationship at each level of each of the factors was calculated using the analysis of variance (ANOVA) methodology. The justification for the selection of this method is that it makes it possible in a simple way to analyse the results and allows a quick conclusion to be drawn. In this work, the interactions between the factors have not been considered, the reason being that having carried out a DOE by Taguchi methodology, the L_9 array does not allow to determine these interactions as it does not have more degrees of freedom.

The S/N relationship indicates the effect of each factor on P removal yield and particle size. As discussed above,

Table 9 Response of S/N relationship for P removal yield and crystal size at pilot scale

Test #	S/N ratio for P removal yield	S/N ratio for crystal size
1	39.07	40.06
2	38.51	40.25
3	38.31	43.30
4	39.81	40.53
5	39.63	41.46
6	39.13	42.43
7	39.82	40.38
8	39.40	40.37
9	39.22	41.75

Table 10 Response of S/N relationship for P removal yield and crystal size

Level	P removal yield				Crystal size			
	Mg/P relation	N/P relation	Air flow ($NL{\cdot}min^{-1}$)	Reaction time (h)	Mg/P relation	N/P relation	Air flow ($NL{\cdot}min^{-1}$)	Reaction time (h)
Level 1	35.60	39.57	39.20	39.31	41.21	40.33	40.95	41.09
Level 2	39.52	37.76	37.76	37.73	41.48	40.69	40.85	41.02
Level 3	39.48	37.28	37.65	37.57	40.84	42.50	41.72	41.40
Delta	3.92	2.28	1.55	1.74	0.64	2.17	0.87	0.38
Rank	1	2	4	3	3	1	2	4

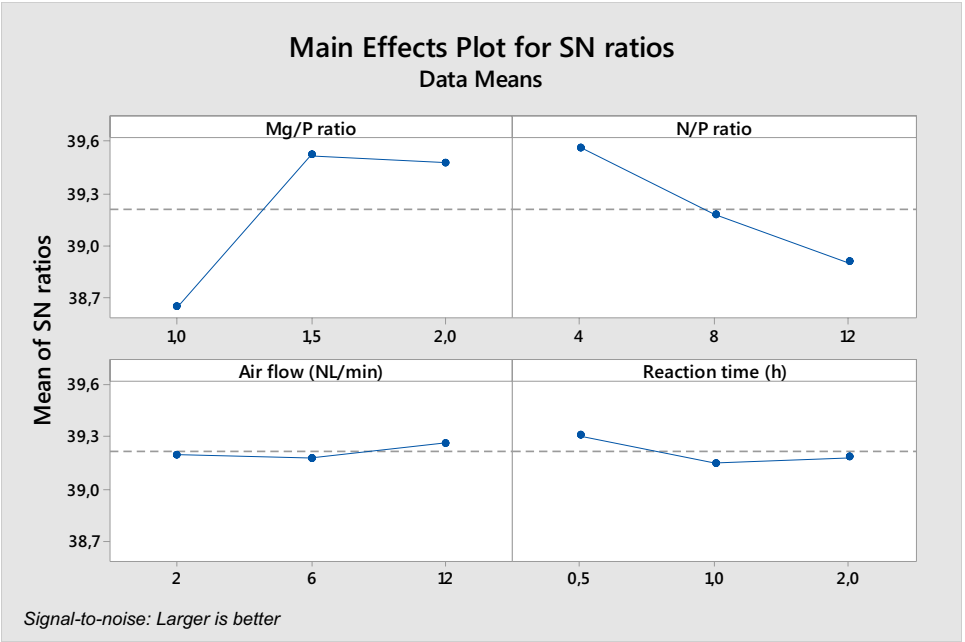

Fig. 10 Effects of process parameters on the P removal yield at pilot scale

for P removal yield and particle size, the S/N relationship is calculated using "larger-better" criteria and the equation for calculating the S/N ratio is shown in Eq. (7).

$$\left(S/N\right) = -10 \cdot \log\left(\frac{1}{n} \cdot \sum_{i=1}^{n} \frac{1}{y_i^2}\right) \quad (7)$$

where n is the number of trials in an experiment, y_i is the experimental response to the i-repetition.

Although there are different criteria for optimising the S/N objective function (larger-better, smaller-better, nominal-better, etc.) it is always interpreted in the same way, i.e. the higher the S/N relationship, the better the result obtained. The range of S/N ratio values (delta) is calculated for each factor and a higher range means a greater influence on P removal performance and particle size.

Effect on P Removal Yield

Table 9 presents the S/N relationship figures for P removal yield and particle size for each experiment.

As specified by Table 10, for the P removal yield, the highest delta value (range width for the different S/Ns of a factor), is the one corresponding to the Mg/P relationship, in the second place of the ranking is find the N/P relationship, then the reaction time and finally the air flow. These results agree with those obtained at the laboratory scale [28]. Therefore, it can be assumed that both the Mg concentration and the P concentration are the parameters that have the greatest effect on the removal yield. The latter can be observed in Fig. 10, since the Mg/P relationship and the N/P relationship are the parameters that have the greatest variation in the S/N as each parameter is changed from one level to another (i.e. these are the parameters with the widest range).

According to the stoichiometry of the struvite crystallisation reaction, 1 mol of Mg reacts with 1 mol of P and 1 mol of N, so it is necessary to work with molar ratios Mg/P = 1.0 or higher [21, 30]. As reported by Lu et al. [31] and Rahaman [32], there is an improvement in the efficiency of P removal by crystallisation with the increment of Mg/P relationship. In the present study, the influence of the Mg/P relationship was evaluated in the range of 1.0–2.0. When the Mg/P relationship was 1.0 (stoichiometric ratio) up to 84% of P removal yields were achieved. However, when the Mg/P relationship was increased from 1.0 to 1.5 or 2.0; the P removal yields were up to 91%. These results agree with those obtained by other authors; as specified by Bhuiyan et al. [29], in FBR reactors, the Mg/P ratio is no longer an influential variable for values higher than 2.0; moreover, Wang et al. [33], obtained an optimal P removal yield for Mg/P relationship of 1.5.

The impact of the N/P relationship on the crystallisation reaction was also studied. For a molar N/P ratio = 4.0, P removal yields of 91% were obtained, however, for higher molar N/P ratios, the obtained P removal yields were significantly lower (up to 90% for N/P ratios = 8.0 and up to 88% for N/P ratios = 12.0). This agrees with the results reported in previous work, where an increase in P removal is achieved as the N/P ratio decreases [31, 34].

The positive effect of increasing reagent concentrations (P and Mg) on the P removal yield is given by the direct relationship between these concentrations and the saturation rate of the reaction [35–38]. The saturation index (SI) is a parameter describing the thermodynamics of the crystallisation reaction, as it behaves as the driving force in the kinetics of struvite precitation. According to Eq. (8), the SI depends on the struvite solubility product ($K_{s(str)}$) and the ionic activity (a_i) of the ions involved in the reaction. According to Hanhoun [39], $K_{s(str)}$ value for struvite can range from $1.15 \cdot 10^{-10}$ to $7.59 \cdot 10^{-14}$ (25 °C). Struvite is considered a slightly soluble salt and therefore ionic activities can be assimilated to ion concentrations.

$$SI = \log\left(\frac{\prod a_i}{K_{S(str)}}\right) = \log\left(\frac{\left[Mg^{2+}\right]\left[NH_4^+\right]\left[HPO_4^{2-}\right][OH^-]}{K_{S(str)}}\right) \quad (8)$$

Knowing the SI value, its thermodynamic state can be defined.

If SI > 0 the solution is supersaturated with struvite.

If SI = 0 the solution is saturated with struvite.

If SI < 0 the solution is not saturated.

On the other hand, Supersaturation (S) can be determined taking into account the SI definition and is usually used in a more common and practical way according to Eq. (9).

$$S = \left(\frac{\prod a_i^{v_i}}{K_{S(str)}}\right)^{1/\nu} = \left(\frac{\left[Mg^{2+}\right]\left[NH_4^+\right]\left[HPO_4^{2-}\right][OH^-]}{K_{S(str)}}\right)^{1/4} \quad (9)$$

υ is the number of total ions in the salt [40].

If S < 1, the solution is not saturated, hence crystallisation does not occur.

If S = 1, the solution is stable for an indefinite period of time, i.e. in the saturated solution, the salt does not thermodynamically tend to generate crystals and on the other hand, the solid particles present in the saturated solution do not dissolve.

If S > 1, the solution will be supersaturated, because there will be an excess of struvite above the solubility and therefore the salt will precipitate.

Logically, as the Mg/P relationship increases and the N/P relationship decreases, the concentrations of P and Mg in the reaction increase, which will encourage the reaction equilibrium to favour struvite precipitation; all this will cause an increase in the yield of the reaction and thus in the P recovery. However, it should be noted that, as already demonstrated at lab scale [29], an excessive increase of the Mg and P concentration in the reaction can lead to a high level of supersaturation that would cause a hindrance in crystal growth and most of them would remain in their primary phase as nuclei [28]. Obviously, a situation of excessive supersaturation in the crystallisation reaction is not desired.

Regarding the effect of the fluidisation air flow rate on the P removal yield, it can be observed that the P removal yield has increased as the air flow rate has increased from 2 to 12 NL·min^{-1}. According to Saidou et al. [41], this may be since air has influenced the P removal efficiency (precipitating as struvite) by increasing the agitation of the reaction medium, which favours the interaction between the different reagents to form the crystal. Authors such as Abarca et al. [26] conclude that P removal increases as the fluidisation rate increases up to a certain value, after which P removal is maintained or even decreases due to the loss of fines. On the other hand, it should be noted that, of all the parameters studied in this work, air flow rate has the least influence on the reaction yield [22, 42]. Finally, it should be noted that the values achieved in the P removal yield in the FBR, with air flow rates between 2 and 12 NL·min^{-1}, were higher or similar to those obtained by mechanical or magnetic stirring (between 69 and 82%) [43, 44].

For the research of the effect of reaction time on the crystallisation reaction, 0.5, 1.0 and 2.0 h were considered. The results showed a P removal yield of more than 80% in most cases. Thus, the effect of reaction time on the crystallisation was very small, especially when the reaction time was

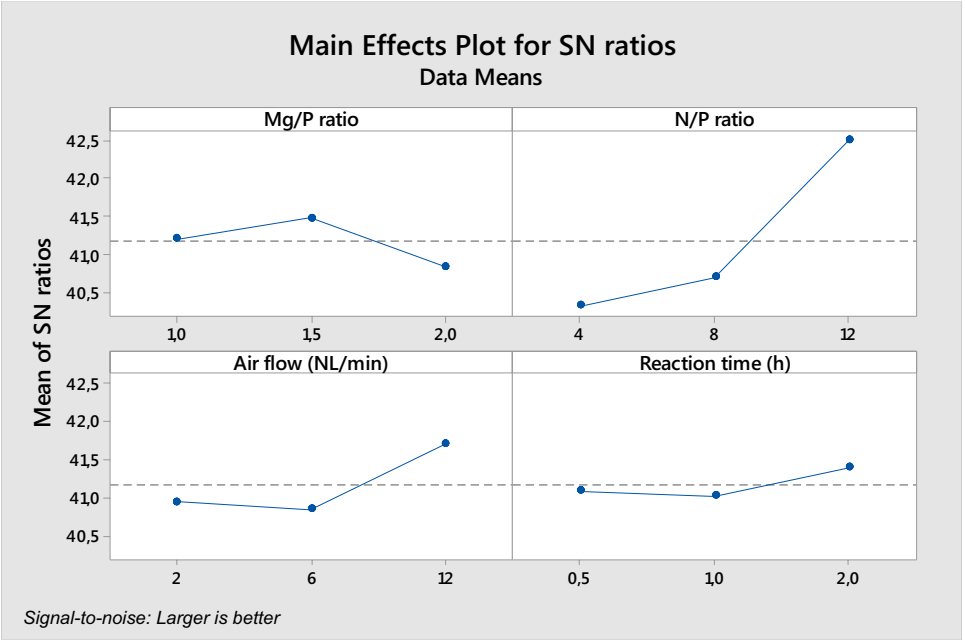

Fig. 11 Effects of process parameters on struvite particle size at pilot scale

incremented from 1.0 to 2.0 h. These results concur with findings of previous works [45–48]. In accordance with Guadie et al. [49], Shih et al. [50] and Shim et al. [51] the increase in P removal via struvite formation for hydraulic retention times (HRT) above 1.0 h was practically negligible.

Influence on Struvite Particle Size

As in the case of the P removal yield, the quantification of the S/N ratio for the crystal size of each test is presented in Table 9. Conforming to the S/N values (Table 10), the N/P relationship is the factor that has the greatest effect on particle size, with a much greater influence than the other three; in second place is the air flow rate, followed by the Mg/P ratio, with a similar influence to the previous one, and finally the reaction time. Figure 11 shows the trends in the particle size effects of the operating parameters.

Rising the concentration of Mg in the solution used in the experiment not only affected the amount of crystals produced, but also had an important influence on the particle size of the struvite. As the Mg concentration, i.e. the Mg/P ratio, increases, the particle diameter is smaller, decreasing from 146 to 104 µm. This effect is very similar in the case of increasing P concentration or, in other words, decreasing N/P ratio. The main reason for this behaviour is mainly to be found in the influence of the supersaturation of the solution. A higher supersaturation, due to an increment in the concentration of the species involved in the struvite precipitation, leads to smaller crystal sizes. This phenomenon occurs by the competition between crystal growth and nucleation. As already discussed in Corona et al. [28], at high supersaturation levels the nucleation rate increases, leading to obtaining a more amount and smaller crystals [40]. In accordance to Ronteltap et al. [52], high initial Mg/P relationships in the reactor lead to high supersaturation levels. This effect is even more noticeable in batch reactions. Moreover, the particle sizes of this work are very similar to those obtained by other authors such as Münch and Barr [53] or Ronteltap et al. [52], all of them being around 100 µm. On the other hand, Le Corre [54] showed that crystal size is restricted by zeta potential of the struvite. Thus, because of its negative zeta potential, crystals do not agglomerate, which prevents larger crystals from forming easily and, therefore, the particle sizes obtained in the experimental development of this chapter are typical for struvite precipitation.

The design of the crystallisation reactor has allowed control of the upward air velocity by controlling the reactor inlet flow rate. This is important since the upward air velocity and, therefore, its flow rate, can influence the crystal size produced at the bottom of the reactor; so that only larger particles with a settling velocity equal to or higher than the upward air velocity can settle to the bottom of the reactor. The results obtained show that the air velocity in the reactor is strongly related with the crystal size of the salt recovered. Thus, the crystal size practically does not vary with the air flow rate from 2 to 6 $L \cdot min^{-1}$, and increases slightly when the air flow rate is increased to 12 $L \cdot min^{-1}$. In general, an increase in the upward air velocity will induce to an increment in nucleation and crystal growth, as mixing of the reactant mass is favoured. In addition, as there is a constant recirculation motion, due to the air pushing the crystal particles at the bottom, they grow as they are transported along the reactor and when they are at the top of the reactor, they fall back by gravity to the bottom of the

reactor. This phenomenon occurs again and again until the crystal is of a certain size and the driving force of the air is not sufficient to overcome the weight of the crystal to lift it. It can therefore be assumed that, in general, an increase in air flow rate will lead to an increase in crystal size. Similarly, high airflow rates lead to more collisions between crystals, which can lead to a high level of compaction of the crystalline aggregate [22]. However, it should be taken into account that when working with low upward velocities, the air could fluidise only a fraction of the crystals, depending on the size of the crystals, which would not allow for a correct growth of the entire available crystal population. The results of Tarragó et al. [42] are in line with the above, since, in that work, an increase in struvite crystal size (from 100 to 240 m) was obtained as the air flow rate increased from 1 to 10 $L{\cdot}min^{-1}$. These results are also consistent with the conclusions of Soare et al. [55] or Zamora et al. [56]. Therefore, the results obtained in the work, regarding the influence of fluidisation air flow rate on particle size are within the expected range.

Finally, an increase in reaction time has generally resulted in crystals with larger particle sizes. The main explanation is that, according to the general behaviour of struvite crystal growth kinetics and reaction conditions favouring saturation; in the first 5–10 min of the reaction, struvite crystals are produced and grow very quickly (up to 50–60 µm), thereafter the crystals continue to grow, but at a much slower rate. The time for the crystals to continue to grow or, on the contrary, to stop growing and reach their final size, depends on the time the crystals are in the metastable phase during their growth and this in turn will depend on the saturation rate of the reaction mixture. These results are in line with previous work [42, 51, 57].

A very decisive factor for the particle size in which the product should be presented for use as fertiliser depends on the nutrient requirements and these in turn will be influenced by agronomic factors such as crop type, soil type, etc. If the product is to be used directly as a fertiliser, it should be ensured that the struvite is present as an aggregate with a minimum particle size. This minimum particle size is mainly determined by the agricultural machinery used for fertilisation (i.e., the fertiliser must have a minimum particle size so that the machine can dose it into the field). Furthermore, it should be taken into account that depending on the particle size of the fertiliser, the solubility of the fertiliser in the soil–plant binomial can vary and therefore improve or worsen the agricultural yield of the fertiliser. If the fertilisation conditions require the addition of other nutrients that are deficient in struvite (such as N or K), the struvite must be blended with these other nutrients and, therefore, it will not be necessary for the starting struvite to have an excessively large particle size. Whether the struvite is to be used directly as a fertiliser or pre-blended with other nutrients, the appropriate size of the final aggregate can be achieved by pelleting.

Effect of Temperature and pH on the Loss of N as NH_3

Based on the results presented in Table 7, it is shown that temperature and pH have a notable influence on ammonia removal. An increment in temperature and pH promotes the releasing of gas-phase N in the form of NH_3. Rising the temperature from 25 to 35 °C and the pH from 9.0 to 10.5 increases the loss of N from the reaction medium in the form of NH_3 from 30 to 90%v. Furthermore, increasing the temperature favours the struvite crystallisation reaction, as it increases the molecular diffusion coefficient of NH_3 in the liquid and gas phases, but, however, causes a significant increase of NH_3 desorption in water, which in turn increases the matter transfer. The results obtained are in line with those suggested by El-Mashad et al. [58] and Huang et al. [59]. Conforming to these authors, the equilibrium between NH_3 and NH_4^+ in an aqueous solution depends on the temperature and pH of the solution and the relation between [NH_3] (g) and [NH_4^+] (ac) can be obtained by the equation proposed by Perry and Chilton [60] Eq. (10), since the amount of NH_3 removed from a solution depends largely on two thermodynamic equilibria: the dissociation equilibrium of liquid ammonia (NH_4^+) and the ammonia-gas–liquid equilibrium.

$$\left[NH_3\right] = \left[NH_4^+\right] \cdot \left(1 + \frac{10^{-pH}}{10^{-\left(0.1075+\left(\frac{2725}{T(K)}\right)\right)}}\right)^{-1} \tag{10}$$

According to Eq. (10), for a pH of 10.5 and a reaction temperature of 35 °C, the loss of N as gaseous NH_3 would be 96%, while at pH 9.0 and 25 °C the loss of N as NH_3 gas would be 36%. These results are therefore very similar to those obtained in this experiment.

Agronomic Potential of Struvite

Regarding the results obtained in the agronomic trial, it can be concluded that both the amount of turf obtained (crop yield) and the height of the turf are very similar in each of the three sectors of the agronomic trial. From the point of view of the nutrient content in the turf, those obtained for the two types of struvite (commercial and experimental) are those with the highest concentration of nutrients (N, Mg and P), to the detriment of the turf obtained from the TF. Furthermore, commercial struvite is the fertiliser with the best results, but very similar to those of the ES obtained in this study. As far as nutrients in the soil are concerned, the lowest amount of nutrients is present in the soil used in the

sowing with TF. In principle, this is more beneficial, since the lower the concentration of nutrients in the soil, the lower the possibility of contamination by leaching. But due to the low leaching that struvite usually has, it ensures that even if the amount of nutrients remaining in the soil is higher for struvite, these will not be lost and will be available at all times for the plant to absorb them as needed. On the other hand, a very positive result for the ES is that, although the concentration of P and Mg is much higher in the starting product compared to the TF, the remaining concentration of these nutrients in the soil is not much higher for the ES soil, which means that the absorption of the nutrients has been better for the ES. However, the negligible difference of remaining nutrients in soil and turf for the two struvites may suggest that the ES works as a slow-release fertiliser in a very similar way to commercial struvite, since both start from practically the same concentration of N, Mg and P and similar nutrient concentrations have been achieved for both in turf and soil. In other words, the turf absorbs the nutrients in a similar way when they come from the two types of struvite.

On the other hand, it should be noted that none of the fertilisers have a notable content of Potentially Toxic Elements (PTEs) or other contaminants [61] that would prevent their use, in accordance with the legislation (Royal Decree 506/2013 and its subsequent amendments); therefore, both soils and crops are free of these elements. Following Kataki et al. [62], in general, struvites from agricultural and livestock waste (as is the case of ES), usually have a lower content of PTEs than struvites from wastewater treatment plants (origin of commercial struvite).

According to Rahman et al. [63], in struvite-treated soil, N losses by leaching are markedly unlike compared to soil treated with chemical fertilisers; therefore, in struvite-fertilised soils, N remains longer in storage and the plant will take up nutrients as needed. The latter is the main virtue of slow-release fertilisers (such as struvite) and, apart from the low N leaching losses, it is also related to the low struvite solubility in water (0.018 g/100 mL at 25 °C, in consonance with Le Corre et al. [64]). According to several authors [63, 65], due to its solubility, struvite can be an effective fertiliser for acid soil and even obtains reasonable efficacies in soils with slightly basic pH [66], being not recommended, however, for calcareous soils. Therefore, struvite can be an interesting P source with renewable origin to use as fertiliser in different soil environments. However, it should be taken into account that the behaviour of the fertiliser will not only be affected by its properties or the properties of the soil where it will be used, but also by the previous management history on that soil [67, 68].

In addition, it should be noted that the high P uptake by the plant is since the application of struvite increases P uptake compared to TF, since the Mg present in struvite has a synergistic effect on P uptake [69–71]. It is important to note that Mg is part of the chlorophyll molecule, this molecule participates in the photosynthesis and encourages the plant growth. Thus, the selling price of struvite could be even higher than that of simple phosphate fertilisers, increasing its economic viability. A very important consideration is the high amount of Mg persisting in the soil. Gell et al. [72] studied the accumulation of Mg in the soil by long-term struvite application, obtaining, in a field trial, a variation of the Ca/Mg ratio of 4–2. According to Kubov et al. [73], Rosanoff et al. [74] and Schulte and Kelling [75], the Ca/Mg ratio in soil can vary from 0.5 to 20, so as not to affect crop yield; when the concentration of Mg in soil becomes notably higher than that of Ca, it can affect hydraulic conductivity, negatively influencing crop yield. Therefore, it is important to monitor the Ca/Mg ratio, since an imbalance between Ca and Mg will lead to a deficit of the first of them in plants [76]. In the case of this study the Ca/Mg mass ratios in the three soils are: 1.08 for the soil fertilised with TF; 1.55 for the commercial struvite soil and 1.01 for the commercial struvite soil, therefore, although the amount of Mg is very similar to that of Ca in all cases, crop yield will not be affected.

Therefore, it can be concluded that the ES presents a good agronomic behaviour (similar to other fertilisers of similar characteristics that are currently available on the market) and that its use as a slow-release biofertiliser can be recommended. Although it is necessary to analyse the scenario in which struvite is to be used (type of soil, type of crop, climatology), as sometimes a crop may be deficient in nutrients such as N or K and in these cases, it will be necessary to use it mixed by blending with other components with fertilising power and which provide the necessary nutrients that struvite is not capable of providing [77]. Finally, it should be noted that the results and conclusions obtained in the agronomic trial are in line with the work carried out by other authors with similar crops. In general, struvite fertilisation equals or even improves the effects of traditional phosphate fertilisers [78–83].

Conclusions

An experimental development has been achieved in a 50 L FBR, Mg concentration, P concentration, flow rate of fluidising agent and reaction time have been selected as parameters to be studied. As pH and temperature, 9.0 and 25 °C were selected for all the experiments, and $MgCl_2 \cdot 6H_2O$ was used as the source of Mg. For each of the four factors studied, three levels were selected, and the Taguchi methodology was applied to determine the DOE, obtaining a reduced factorial L_9.

As for the results obtained from the statistical analysis associated with the design of experiments, it is concluded that the concentrations of P and Mg in the reaction medium are the parameters that most influence the yield of the struvite crystallisation reaction Therefore, the higher the Mg and P concentrations, the higher the P removal yield; however, it should be taken into account that when working with very high concentrations, the phenomenon of supersaturation will be favoured. Very high values of supersaturation (> 20) will lead to a decrease in crystal size and therefore in the reaction yield. The latter is due to the fact that the correct nucleation and growth of most of the nuclei or embryos formed during the reaction process does not occur [28]. Thus, the optimum level for the Mg/P relationship are 1.5 and for the N/P relationship 4.0. On the other hand, the air flow rate of the fluidising agent has the least effect on the P removal yield. Therefore, moderate air flow rates would be sufficient for a correct development of the struvite crystallisation reaction. It is required to work with a minimum air flow rate to produce fluidisation and favour the contact and mixing of the reacting mass, but trying to avoid phenomena of dragging of fines, which entails a loss of crystals in the initial phases of their growth, due to an excessively high fluidisation speed. With respect to the reaction time, this also has a minor influence on the crystallisation reaction, within the range of the study (between 0.5 and 2.0 h). Therefore, reaction times between 0.5 and 1.0 h are sufficient to achieve high reaction yields.

As far as crystal size is concerned, in addition to the aforementioned negative influence that Mg and P concentrations can cause, due to the phenomenon of excessive supersaturation, the increase in reaction time contributes positively to the increase in particle size, since, according to the kinetics of the crystal, it increases in size over the course of the reaction, The particles grow very fast in the first few minutes of the reaction and then increase much more slowly, with almost no difference in size between the crystals obtained after 1.0 h of reaction and those obtained after 2.0 h. In addition, the air flow rate introduced into the FBR will also have a positive effect on the particle size, in such a way that the increase in the flow rate will favour obtaining larger particles; however, an excessive increment in the air flow rate can produce the dragging of the fines or crystal nuclei that are being formed and prevent them from growing correctly, having an average population of crystals with a smaller particle size.

Nevertheless, it is crucial to highlight that, thanks to the study carried out in this work, high pH values and reaction temperature leads to an increment in the P removal yield, but, on the contrary, result in an increment in the loss of N in the form of NH_3 gas (due to the displacement of the NH_4^+/NH_3 equilibrium). For that reason, it is not advisable to carry out crystallisation reactions at pH values higher than 9.0–9.5 or temperatures of 25–30 °C.

Finally, the agronomic potential of the struvite obtained in these experiments has been demonstrated in field trials for turf growth. In these trials, the results obtained for struvite were very similar to those obtained for commercial struvite and considerably better than those obtained for a TF.

Acknowledgements This work was supported by the European Commission through the Grant Agreement ID: 773682 (NUTRI2CYCLE project) and by the Agencia de Innovación, Financiación e Internacionalización Empresarial de Castilla y León (Economía circular en el sector agroalimentario ADE_ECOCIR project).

Author Contributions FC conducted the experimental part of the study. DH directed, coordinated and organised the experimental study. She also defined the DOE to be carried out in Spain and coordinated with GA the discussion of results and conclusions of the work. JMM participated in the experimental development and collaborated in the analysis of the samples and the implementation of the analytical techniques. JC participated in the experimental development and collaborated in the analysis of the samples and the implementation of the analytical techniques. SS participated in the experimental development. GA directed, coordinated and organised the experimental study in close collaboration with DH. He also defined the DOE and coordinated with DH the discussion of results and conclusions of the work.

Funding This work has received funding from the European Commission through the Grant Agreement ID: 773682 (NUTRI2CYCLE project) and by the Agencia de Innovación, Financiación e Internacionalización Empresarial de Castilla y León (project: Economía circular en el sector agroalimentario ADE_ECOCIR).

Data Availability All requests for raw and analysed data and materials will be made available upon reasonable academic request within the limitations of informed consent by the corresponding author upon acceptance.

Declarations

Conflict of interest The authors declare that they have no conflict of interest.

References

1. Hu, L., Yu, J., Luo, H., Wang, H., Xu, P., Zhang, Y.: Simultaneous recovery of ammonium, potassium and magnesium from produced

water by struvite precipitation. Chem. Eng. J. **382**, 123001 (2020). https://doi.org/10.1016/j.cej.2019.123001
2. Lorick, D., Macura, B., Ahlström, M., Grimvall, A., Harder, R.: Effectiveness of struvite precipitation and ammonia stripping for recovery of phosphorus and nitrogen from anaerobic digestate: a systematic review. Environ. Evid. **9**(1), 1–20 (2020). https://doi.org/10.1186/s13750-020-00211-x
3. Mavhungu, A., Foteinis, S., Mbaya, R., Masindi, V., Kortidis, I., Mpenyana-Monyatsi, L., Chatzisymeon, E.: Environmental sustainability of municipal wastewater treatment through struvite precipitation: influence of operational parameters. J. Clean. Prod. **285**, 124856 (2021). https://doi.org/10.1016/j.jclepro.2020.124856
4. Siciliano, A., Limonti, C., Curcio, G.M., Molinari, R.: Advances in struvite precipitation technologies for nutrients removal and recovery from aqueous waste and wastewater. Sustainability **12**(18), 7538 (2020). https://doi.org/10.3390/su12187538
5. Sun, H., Mohammed, A.N., Liu, Y.: Phosphorus recovery from source-diverted blackwater through struvite precipitation. Sci. Total Environ. **743**, 140747 (2020). https://doi.org/10.1016/j.scitotenv.2020.140747
6. Schneider, P.A., Wallace, J.W., Tickle, J.C.: Modelling and dynamic simulation of struvite precipitation from source-separated urine. Water Sci. Technol. **67**(12), 2724–2732 (2013). https://doi.org/10.2166/wst.2013.184
7. Ye, Z., Shen, Y., Ye, X., Zhang, Z., Chen, S., Shi, J.: Phosphorus recovery from wastewater by struvite crystallization: property of aggregates. J. Environ. Sci. **26**(5), 991–1000 (2014). https://doi.org/10.1016/S1001-0742(13)60536-7
8. Ghosh, S., Lobanov, S., Lo, V.K.: An overview of technologies to recover phosphorus as struvite from wastewater: advantages and shortcomings. Environ. Sci. Pollut. Res. **26**(19), 19063–19077 (2019). https://doi.org/10.1007/s11356-019-05378-6
9. Santiviago, C., Peralta, J., López, I.: Phosphorus removal from wastewater through struvite crystallization in a continuous fluidized-bed reactor: an improved comprehensive model. Chem. Eng. J. **430**, 132903 (2022). https://doi.org/10.1016/j.cej.2021.132903
10. Desmidt, E., Ghyselbrecht, K., Zhang, Y., Pinoy, L., Van der Bruggen, B., Verstraete, W., Rabaey, K., Meesschaert, B.: Global phosphorus scarcity and full-scale P-recovery techniques: a review. Crit. Rev. Environ. Sci. Technol. **45**(4), 336–384 (2015). https://doi.org/10.1080/10643389.2013.866531
11. Fattah, K.P., Mavinic, D.S., Koch, F.A.: Influence of process parameters on the characteristics of struvite pellets. J. Environ. Eng. **138**(12), 1200–1209 (2012). https://doi.org/10.1061/(ASCE)EE.1943-7870.0000576
12. Le Corre, K.S., Valsami-Jones, E., Hobbs, P., Jefferson, B., Parsons, S.A.: Struvite crystallisation and recovery using a stainless steel structure as a seed material. Water Res. **41**(11), 2449–2456 (2007). https://doi.org/10.1016/j.watres.2007.03.002
13. Lougheed, T.: Phosphorus recovery: new approaches to extending the life cycle. Environ. Health Perspect. **119**(7), 302–305 (2011). https://doi.org/10.1289/ehp.119-a302
14. Fattah, K.P.: Assessing struvite formation potential at wastewater treatment plants. Int. J. Environ. Sci. Dev. **3**(6), 548 (2012). https://doi.org/10.7763/IJESD.2012.V3.284
15. Adnan, A., Dastur, M., Mavinic, D.S., Koch, F.A.: Preliminary investigation into factors affecting controlled struvite crystallization at the bench scale. J. Environ. Eng. Sci. **3**(3), 195–202 (2004). https://doi.org/10.1139/s03-082
16. Battistoni, P., De Angelis, A., Prisciandaro, M., Boccadoro, R., Bolzonella, D.: P removal from anaerobic supernatants by struvite crystallization: long term validation and process modelling. Water Res. **36**(8), 1927–1938 (2002). https://doi.org/10.1016/S0043-1354(01)00401-8
17. Mehta, C.M., Batstone, D.J.: Nucleation and growth kinetics of struvite crystallization. Water Res. **47**(8), 2890–2900 (2013). https://doi.org/10.1016/j.watres.2013.03.007
18. Rahaman, M.M., Salleh, M.A.M., Rashid, U., Ahsan, A., Hossain, M.M., Ra, C.S.: Production of slow release crystal fertilizer from wastewaters through struvite crystallization—a review. Arab. J. Chem. **7**(1), 139–155 (2014). https://doi.org/10.1016/j.arabjc.2013.10.007
19. Fromberg, M., Pawlik, M., Mavinic, D.S.: Induction time and zeta potential study of nucleating and growing struvite crystals for phosphorus recovery improvements within fluidized bed reactors. Powder Technol. **360**, 715–730 (2020). https://doi.org/10.1016/j.powtec.2019.09.067
20. Li, B., Boiarkina, I., Yu, W., Huang, H.M., Munir, T., Wang, G.Q., Young, B.R.: Phosphorous recovery through struvite crystallization: challenges for future design. Sci. Total Environ. **648**, 1244–1256 (2019). https://doi.org/10.1016/j.scitotenv.2018.07.166
21. Li, B., Huang, H.M., Boiarkina, I., Yu, W., Huang, Y.F., Wang, G.Q., Young, B.R.: Phosphorus recovery through struvite crystallisation: recent developments in the understanding of operational factors. J. Environ. Manag. **248**, 109254 (2019). https://doi.org/10.1016/j.jenvman.2019.07.025
22. Ye, X., Ye, Z.L., Lou, Y., Pan, S., Wang, X., Wang, M.K., Chen, S.: A comprehensive understanding of saturation index and upflow velocity in a pilot-scale fluidized bed reactor for struvite recovery from swine wastewater. Powder Technol. **295**, 16–26 (2016). https://doi.org/10.1016/j.powtec.2016.03.022
23. Capdevielle, A., Sýkorová, E., Biscans, B., Béline, F., Daumer, M.L.: Optimization of struvite precipitation in synthetic biologically treated swine wastewater—determination of the optimal process parameters. J. Hazard. Mater. **244**, 357–369 (2013). https://doi.org/10.1016/j.jhazmat.2012.11.054
24. Uysal, A., Kuru, B.: Examination of nutrient removal from anaerobic effluent of the dairy processing industry by struvite precipitation using the response surface methodology. Fresenius Environ. Bull. **22**(5), 1380–1387 (2013)
25. Ye, Z.L., Chen, S.H., Wang, S.M., Lin, L.F., Yan, Y.J., Zhang, Z.J., Chen, J.S.: Phosphorus recovery from synthetic swine wastewater by chemical precipitation using response surface methodology. J. Hazard. Mater. **176**(1–3), 1083–1088 (2010). https://doi.org/10.1016/j.jhazmat.2009.10.129
26. Abarca, R.R.M., Pusta, R.S., Jr., Labad, R.B., Andit, J.L.A., Rejas, C.M., de Luna, M.D.G., Lu, M.C.: Effect of upflow velocity on nutrient recovery from swine wastewater by fluidized bed struvite crystallization. In: Chemistry and Water, pp. 511–518. Elsevier, Amsterdam (2017). https://doi.org/10.1016/B978-0-12-809330-6.00014-3
27. Xu, K., Ge, L., Wang, C.: Effect of upflow velocity on the performance of a fluidized bed reactor to remove phosphate from simulated swine wastewater. Int. Biodeterior. Biodegradation **140**, 78–83 (2019). https://doi.org/10.1016/j.ibiod.2019.03.015
28. Corona, F., Hidalgo, D., Martín-Marroquín, J.M., Antolín, G.: Study of the influence of the reaction parameters on nutrients recovering from digestate by struvite crystallisation. Environ. Sci. Pollut. Res. (2021). https://doi.org/10.1007/s11356-020-08400-4
29. Bhuiyan, M.I.H., Mavinic, D.S., Koch, F.A.: Phosphorus recovery from wastewater through struvite formation in fluidized bed reactors: a sustainable approach. Water Sci. Technol. **57**(2), 175–181 (2008). https://doi.org/10.2166/wst.2008.002
30. Rodrigues, D.M., do Amaral Fragoso, R., Carvalho, A.P., Hein, T., Guerreiro de Brito, A.: Recovery of phosphates as struvite from urine-diverting toilets: optimization of pH, Mg:PO_4 ratio and contact time to improve precipitation yield and crystal morphology. Water Sci. Technol. **80**(7), 1276–1286 (2019). https://doi.org/10.2166/wst.2019.371

31. Lu, B., Xu, J., Zhang, M., Pang, W., Xie, L.: Phosphorus removal and recovery from wastewater by highly efficient struvite crystallization in an improved fluidized bed reactor. Korean J. Chem. Eng. **34**(11), 2879–2885 (2017). https://doi.org/10.1007/s11814-017-0203-1
32. Rahaman, M.: Phosphorus recovery from wastewater through struvite crystallization in a fluidized bed reactor: kinetics, hydrodynamics and performance (Doctoral dissertation, University of British Columbia) (2009). https://doi.org/10.14288/1.0072391
33. Wang, J., Ye, X., Zhang, Z., Ye, Z.L., Chen, S.: Selection of cost-effective magnesium sources for fluidized struvite crystallization. J. Environ. Sci. **70**, 144–153 (2018). https://doi.org/10.1007/s11814-017-0203-1
34. Guadie, A., Xia, S., Jiang, W., Zhou, L., Zhang, Z., Hermanowicz, S.W., Xu, X., Shen, S.: Enhanced struvite recovery from wastewater using a novel cone-inserted fluidized bed reactor. J. Environ. Sci. **26**(4), 60469–60476 (2014). https://doi.org/10.1016/S1001-0742(13)60469-6
35. Edahwati, L.: The effect of supersaturation control strategy For phosphate recovery through precipitation Of struvite in an air-agitated column reactor. Rasayan J. Chem. 11(2) 904-914 (2018). https://doi.org/10.31788/RJC.2018.1123007
36. Elduayen-Echave, B., Azcona, M., Grau, P., Schneider, P.A.: Effect of the shear rate and supersaturation on the nucleation and growth of struvite in batch stirred tank reactors. J. Water Process Eng. **38**, 101657 (2020). https://doi.org/10.1016/j.jwpe.2020.101657
37. Le, V.G., Vo, D.V.N., Nguyen, N.H., Shih, Y.J., Vu, C.T., Liao, C.H., Huang, Y.H.: Struvite recovery from swine wastewater using fluidized-bed homogeneous granulation process. J. Environ. Chem. Eng. **9**(3), 105019 (2021). https://doi.org/10.1016/j.jece.2020.105019
38. Wang, Y., Mou, J., Liu, X., Chang, J.: Phosphorus recovery from wastewater by struvite in response to initial nutrients concentration and nitrogen/phosphorus molar ratio. Sci. Total Environ. **789**, 147970 (2021). https://doi.org/10.1016/j.scitotenv.2021.147970
39. Hanhoun, M., Montastruc, L., Azzaro-Pantel, C., Biscans, B., Frèche, M., Pibouleau, L.: Temperature impact assessment on struvite solubility product: a thermodynamic modeling approach. Chem. Eng. J. **167**(1), 50–58 (2011). https://doi.org/10.1016/j.cej.2010.12.001
40. Mullin, J.W.: Crystallization. Elsevier, Amsterdam (2004)
41. Saidou, H., Korchef, A., Moussa, S.B., Amor, M.B.: Struvite precipitation by the dissolved CO_2 degasification technique: impact of the airflow rate and pH. Chemosphere **74**(2), 338–343 (2009). https://doi.org/10.1016/j.chemosphere.2008.09.081
42. Tarragó, E., Puig, S., Ruscalleda, M., Balaguer, M.D., Colprim, J.: Controlling struvite particles' size using the up-flow velocity. Chem. Eng. J. **302**, 819–827 (2016). https://doi.org/10.1016/j.cej.2016.06.036
43. Ichihashi, O., Hirooka, K.: Removal and recovery of phosphorus as struvite from swine wastewater using microbial fuel cell. Bioresour. Technol. **114**, 303–307 (2012). https://doi.org/10.1016/j.biortech.2012.02.124
44. Quintana, M., Colmenarejo, M.F., Barrera, J., Sánchez, E., García, G., Travieso, L., Borja, R.: Removal of phosphorus through struvite precipitation using a by-product of magnesium oxide production (BMP): effect of the mode of BMP preparation. Chem. Eng. J. **136**(2–3), 204–209 (2008). https://doi.org/10.1016/j.cej.2007.04.002
45. Lahav, O., Telzhensky, M., Zewuhn, A., Gendel, Y., Gerth, J., Calmano, W., Birnhack, L.: Struvite recovery from municipal-wastewater sludge centrifuge supernatant using seawater NF concentrate as a cheap Mg(II) source. Sep. Purif. Technol. **108**, 103–110 (2013). https://doi.org/10.1016/j.seppur.2013.02.002
46. Le Corre, K.S., Valsami-Jones, E., Hobbs, P., Parsons, S.A.: Impact of reactor operation on success of struvite precipitation from synthetic liquors. Environ. Technol. **28**(11), 1245–1256 (2007). https://doi.org/10.1080/09593332808618885
47. Liu, Z., Zhao, Q., Lee, D.J., Yang, N.: Enhancing phosphorus recovery by a new internal recycle seeding MAP reactor. Bioresour. Technol. **99**(14), 6488–6493 (2008). https://doi.org/10.1016/j.biortech.2007.11.039
48. Pastor, L., Mangin, D., Ferrer, J., Seco, A.: Struvite formation from the supernatants of an anaerobic digestion pilot plant. Bioresour. Technol. **101**(1), 118–125 (2010). https://doi.org/10.1016/j.biortech.2009.08.002
49. Guadie, A., Xia, S., Zhang, Z., Guo, W., Ngo, H.H., Hermanowicz, S.W.: Simultaneous removal of phosphorus and nitrogen from sewage using a novel combo system of fluidized bed reactor–membrane bioreactor (FBR–MBR). Bioresour. Technol. **149**, 276–285 (2013). https://doi.org/10.1016/j.biortech.2013.09.007
50. Shih, Y.J., Abarca, R.R.M., de Luna, M.D.G., Huang, Y.H., Lu, M.C.: Recovery of phosphorus from synthetic wastewaters by struvite crystallization in a fluidized-bed reactor: effects of pH, phosphate concentration and coexisting ions. Chemosphere **173**, 466–473 (2017). https://doi.org/10.1016/j.chemosphere.2017.01.088
51. Shim, S., Won, S., Reza, A., Kim, S., Ahmed, N., Ra, C.: Design and optimization of fluidized bed reactor operating conditions for struvite recovery process from swine wastewater. Processes **8**(4), 422 (2020). https://doi.org/10.3390/pr8040422
52. Ronteltap, M., Maurer, M., Hausherr, R., Gujer, W.: Struvite precipitation from urine–influencing factors on particle size. Water Res. **44**(6), 2038–2046 (2010). https://doi.org/10.1016/j.watres.2009.12.015
53. Münch, E.V., Barr, K.: Controlled struvite crystallisation for removing phosphorus from anaerobic digester sidestreams. Water Res. **35**(1), 151–159 (2001). https://doi.org/10.1016/S0043-1354(00)00236-0
54. Le Corre, K.S.: Understanding struvite crystallisation and recovery. (2006). https://dspace.lib.cranfield.ac.uk/bitstream/handle/1826/1434/Kristell%20Le%20Corre%20PhD%20thesis%20-05-02-07.pdf?sequence=1. Accessed 20 May 2020.
55. Soare, A., Lakerveld, R., van Royen, J., Zocchi, G., Stankiewicz, A.I., Kramer, H.J.: Minimization of attrition and breakage in an airlift crystallizer. Ind. Eng. Chem. Res. **51**(33), 10895–10909 (2012). https://doi.org/10.1021/ie300432w
56. Zamora, P., Georgieva, T., Salcedo, I., Elzinga, N., Kuntke, P., Buisman, C.J.: Long-term operation of a pilot-scale reactor for phosphorus recovery as struvite from source-separated urine. J. Chem. Technol. Biotechnol. **92**(5), 1035–1045 (2017). https://doi.org/10.1002/jctb.5079
57. Fang, C., Zhang, T., Jiang, R., Ohtake, H.: Phosphate enhance recovery from wastewater by mechanism analysis and optimization of struvite settleability in fluidized bed reactor. Sci. Rep. **6**, 32215 (2016). https://doi.org/10.1038/srep32215
58. El-Mashad, H.M., Zeeman, G., Van Loon, W.K., Bot, G.P., Lettinga, G.: Effect of temperature and temperature fluctuation on thermophilic anaerobic digestion of cattle manure. Bioresour. Technol. **95**(2), 191–201 (2004). https://doi.org/10.1016/j.biortech.2003.07.013
59. Huang, H., Guo, G., Zhang, P., Zhang, D., Liu, J., Tang, S.: Feasibility of physicochemical recovery of nutrients from swine wastewater: evaluation of three kinds of magnesium sources. J. Taiwan Inst. Chem. Eng. **70**, 209–218 (2017). https://doi.org/10.1016/j.jtice.2016.10.051
60. Perry, R.H., Chilton, C.H.: Chemical Engineers Handbook, 5th edn. McGraw-Hill, New York (1973)
61. Wang, Y., Deng, Y., Liu, X., Chang, J.: Adsorption behaviors and reduction strategies of heavy metals in struvite recovered from

swine wastewater. Chem. Eng. J. **437**, 135288 (2022). https://doi.org/10.1016/j.cej.2022.135288
62. Kataki, S., West, H., Clarke, M., Baruah, D.C.: Phosphorus recovery as struvite: recent concerns for use of seed, alternative Mg source, nitrogen conservation and fertilizer potential. Resour. Conserv. Recycl. **107**, 142–156 (2016). https://doi.org/10.1016/j.resconrec.2015.12.009
63. Rahman, M.M., Liu, Y., Kwag, J.H., Ra, C.: Recovery of struvite from animal wastewater and its nutrient leaching loss in soil. J. Hazard. Mater. **186**(2–3), 2026–2030 (2011). https://doi.org/10.1016/j.jhazmat.2010.12.103
64. Le Corre, K.S., Valsami-Jones, E., Hobbs, P., Parsons, S.A.: Phosphorus recovery from wastewater by struvite crystallization: a review. Crit. Rev. Environ. Sci. Technol. **39**(6), 433–477 (2009). https://doi.org/10.1080/10643380701640573
65. Johnston, A.E., Richards, I.R.: Effectiveness of different precipitated phosphates as phosphorus sources for plants. Soil Use Manag. **19**(1), 45–49 (2003). https://doi.org/10.1111/j.1475-2743.2003.tb00278.x
66. Massey, M.S., Davis, J.G., Ippolito, J.A., Sheffield, R.E.: Effectiveness of recovered magnesium phosphates as fertilizers in neutral and slightly alkaline soils. Agron. J. **101**(2), 323–329 (2009). https://doi.org/10.2134/agronj2008.0144
67. Anderson, R., Brye, K.R., Greenlee, L., Gbur, E.: Chemically precipitated struvite dissolution dynamics over time in various soil textures. Agric. Sci. **11**(06), 567–591 (2020)
68. Anderson, R., Brye, K.R., Kekedy-Nagy, L., Greenlee, L., Gbur, E., Roberts, T.L.: Total extractable phosphorus in flooded soil as affected by struvite and other fertilizer-phosphorus sources. Soil Sci. Soc. Am. J. **85**(4), 1157–1173 (2021). https://doi.org/10.1002/saj2.20237
69. Bastida, F., Jehmlich, N., Martínez-Navarro, J., Bayona, V., García, C., Moreno, J.L.: The effects of struvite and sewage sludge on plant yield and the microbial community of a semiarid Mediterranean soil. Geoderma **337**, 1051–1057 (2019). https://doi.org/10.1016/j.geoderma.2018.10.046
70. González-Ponce, R., López-de-Sá, E.G., Plaza, C.: Lettuce response to phosphorus fertilization with struvite recovered from municipal wastewater. HortScience **44**(2), 426–430 (2009). https://doi.org/10.21273/HORTSCI.44.2.426
71. Lustosa Filho, J.F., Penido, E.S., Castro, P.P., Silva, C.A., Melo, L.C.: Co-pyrolysis of poultry litter and phosphate and magnesium generates alternative slow-release fertilizer suitable for tropical soils. ACS Sustain. Chem. Eng. **5**(10), 9043–9052 (2017). https://doi.org/10.1021/acssuschemeng.7b01935
72. Gell, K., De Ruijter, F.J., Kuntke, P., De Graaff, M., Smit, A.L.: Safety and effectiveness of struvite from black water and urine as a phosphorus fertilizer. J. Agric. Sci. **3**(3), 67 (2011). https://doi.org/10.5539/jas.v3n3p67
73. Kubov, M., Schieber, B., Janík, R.: Seasonal dynamics of macronutrients in aboveground biomass of two herb-layer species in a beech forest. Biologia **74**(11), 1415–1424 (2019). https://doi.org/10.2478/s11756-019-00317-9
74. Rosanoff, A., Capron, E., Barak, P., Mathews, B., Nielsen, F.: Edible plant tissue and soil calcium: magnesium ratios: data too sparse to assess implications for human health. Crop Pasture Sci. **66**(12), 1265–1277 (2016). https://doi.org/10.1071/CP15085
75. Schulte, E.E., Kelling, K.A.: Soil Calcium to Magnesium Ratios—should You be Concerned? University of Wisconsin—Extension, Madison (2004)
76. Stevens, G., Gladbach, T., Motavalli, P., Dunn, D.: Soil calcium: magnesium ratios and lime recommendations for cotton. J. Cotton Sci. **9**, 65–71 (2005)
77. Valle, S.F., Giroto, A.S., Guimarães, G.G., Nagel, K.A., Galinski, A., Cohnen, J., Jablonowski N.D., Ribeiro, C.: Co-fertilization of sulfur and struvite-phosphorus in a slow-release fertilizer improves soybean cultivation. (2021). https://doi.org/10.26434/chemrxiv-2021-rv2lh
78. Achat, D.L., Sperandio, M., Daumer, M.L., Santellani, A.C., Prud'Homme, L., Akhtar, M., Morel, C.: Plant-availability of phosphorus recycled from pig manures and dairy effluents as assessed by isotopic labeling techniques. Geoderma **232**, 24–33 (2014). https://doi.org/10.1016/j.geoderma.2014.04.028
79. Ahmed, N., Shim, S., Won, S., Ra, C.: Struvite recovered from various types of wastewaters: characteristics, soil leaching behaviour, and plant growth. Land Degrad. Dev. **29**(9), 2864–2879 (2018). https://doi.org/10.1002/ldr.3010
80. Bonvin, C., Etter, B., Udert, K.M., Frossard, E., Nanzer, S., Tamburini, F., Oberson, A.: Plant uptake of phosphorus and nitrogen recycled from synthetic source-separated urine. Ambio **44**(2), 217–227 (2015). https://doi.org/10.1007/s13280-014-0616-6
81. Omidire, N.S., Brye, K.R., Roberts, T.L., Kekedy-Nagy, L., Greenlee, L., Gbur, E.E., Mozzoni, L.A.: Evaluation of electrochemically precipitated struvite as a fertilizer-phosphorus source in flood-irrigated rice. Agron. J. **114**(1), 739–755 (2022). https://doi.org/10.1002/agj2.20917
82. Reza, A., Shim, S., Kim, S., Ahmed, N., Won, S., Ra, C.: Nutrient leaching loss of pre-treated struvite and its application in Sudan grass cultivation as an eco-friendly and sustainable fertilizer source. Sustainability **11**(15), 4204 (2019). https://doi.org/10.3390/su11154204
83. Szymańska, M., Szara, E., Wąs, A., Sosulski, T., van Pruissen, G.W., Cornelissen, R.L.: Struvite—an innovative fertilizer from anaerobic digestate produced in a bio-refinery. Energies **12**(2), 296 (2019). https://doi.org/10.3390/en12020296